Direct Observation of Coupling between Structural Fluctuation and Ultrafast Hydration Dynamics of Fluorescent Probes in Anionic Micelles

ARTICLE *in* THE JOURNAL OF PHYSICAL CHEMISTRY B · APRIL 2015

Impact Factor: 3.3 · DOI: 10.1021/jp511899q

7 AUTHORS, INCLUDING:

Susobhan Choudhury
S.N. Bose National Centre for Basic Sciences
9 PUBLICATIONS **20** CITATIONS
SEE PROFILE

Prasanna Kumar Mondal
Belgian Nuclear Research Centre
19 PUBLICATIONS **49** CITATIONS
SEE PROFILE

Veerendra Sharma
Solid State Physics Division
12 PUBLICATIONS **18** CITATIONS
SEE PROFILE

Ramaprosad Mukhopadhyay
Bhabha Atomic Research Centre
152 PUBLICATIONS **978** CITATIONS
SEE PROFILE

THE JOURNAL OF PHYSICAL CHEMISTRY B

Article

pubs.acs.org/JPCB

Direct Observation of Coupling between Structural Fluctuation and Ultrafast Hydration Dynamics of Fluorescent Probes in Anionic Micelles

Susobhan Choudhury,[†] Prasanna Kumar Mondal,[†] V. K. Sharma,[‡] S. Mitra,[‡] V. Garcia Sakai,[§] R. Mukhopadhyay,[‡] and Samir Kumar Pal*[,†]

[†]Department of Chemical, Biological & Macromolecular Sciences, S. N. Bose National Centre for Basic Sciences, Block JD, Sector III, Salt Lake, Kolkata 700 098, India

[‡]Solid State Physics Division, Bhabha Atomic Research Centre, Mumbai 400085, India

[§]Science and Technology Facilities Council, Rutherford Appleton Laboratory, Didcot, OX11 0QX, U.K.

ABSTRACT: The coupling of structural fluctuation and the dynamics of associated water molecules of biological macromolecules is vital for various biological activities. Although a number of molecular dynamics (MD) studies on proteins/DNA predicted the importance of such coupling, experimental evidence of variation of hydration dynamics with controlled structural fluctuation even in model macromolecule is sparse and raised controversies in the contemporary literature. Here, we have investigated dynamics of hydration at the surfaces of two similar anionic micelles sodium dodecyl sulfate (SDS) and sodium dodecylbenzenesulfonate (SDBS) as model macromolecules using coumarin 500 (C500) as spectroscopic probe with femtosecond to picosecond time resolution up to 20 ns time window. The constituting surfactants SDS and SDBS are structurally similar except one benzene moiety in the SDBS may offer additional rigidity to the SDBS micelles through π-stacking and added bulkiness. The structural integrity of the micelles in the aqueous medium is confirmed in dynamic light scattering (DLS) studies. A variety of studies including polarization gated fluorescence spectroscopy and quasielastic neutron scattering (QENS) have been used to confirm differential structural fluctuation of SDS and SDBS micelles. We have also employed femtosecond-resolved Förster resonance energy transfer (FRET) in order to study binding of a cationic organic ligand ethidium bromide (EtBr) salt at the micellar surfaces. The distance distribution of the donor (C500)−acceptor (EtBr) in the micellar media reveals the manifestation of the structural flexibility of the micelles. Our studies on dynamical coupling of the structural flexibility with surface hydration in the nanoscopic micellar media may find the relevance in the "master−slave" type water dynamics in biologically relevant macromolecules.

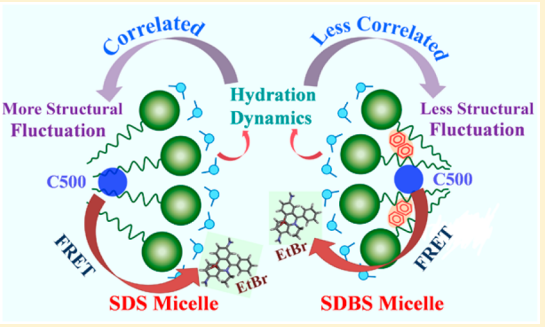

INTRODUCTION

Exchange of dynamical information between biological macromolecules and water molecules in their vicinity (hydration water) is found to be key for the biological function of water as the "matrix of life".[1−4] The ubiquitous dynamical role of hydration water in various biological processes including charge transfer,[5−7] productive enzyme substrate complex formation,[8,9] and protein folding[10,11] is well documented in the early and recent literature. Master role of water molecules at surface[12] and interior[13] of biologically relevant macromolecules in the control of macromolecular dynamics has also been proposed. Whereas the influence of hydration water on the dynamics and function of several biologically relevant macromolecules is evidenced[14] and believed to be slave to those of the solvent, yet to date, how dynamical coupling between the hydration water and biologically relevant macromolecules occurs remains unclear.[15−18] This is because of experimental difficulties in directly accessing hydration water dynamics.[15,19] The usefulness of femtosecond resolved electronic spectroscopy in the exploration of the dynamics of hydration in various biological macromolecules is evidenced and reviewed.[14,20]

In the present work we have used two anionic micelles sodium dodecyl sulfate (SDS; $C_{12}H_{25}SO_4Na$) and sodium dodecylbenzenesulfonate (SDBS; $C_{12}H_{25}C_6H_4SO_3Na$) as model macromolecule. SDBS monomer has the same alkyl moiety as SDS with an extra phenyl ring linked to a sulfonate group. Although SDBS and SDS micelles are very similar from a structural point of view, their dynamical behavior differs significantly. Dynamic light scattering (DLS) studies confirm structural integrity of the micelles in our experimental condition. Recent molecular dynamics[21] studies clearly show that the dynamics of SDBS micelles are more restricted compared to SDS micelles. The structure factor indicates that

Special Issue: Biman Bagchi Festschrift

Received: November 29, 2014
Revised: April 8, 2015

DOI: 10.1021/jp511899q
J. Phys. Chem. B XXXX, XXX, XXX−XXX

the alkyl chains are more flexible in SDS compared with SDBS.[22] The restricted structural flexibility of the SDBS micelles is believed to be due to the π-stacking of two benzene moieties of two adjacent surfactants,[23] though other possibilities including increase in the molar mass of SDBS cannot be completely ruled out. Results of our QENS study reveal restricted internal motion in the case of SDBS micelle compared to that of the SDS micelle.

We have employed temperature dependent polarization gated fluorescence anisotropy of a well-known fluorescence probe coumarin 500 (C500)[24] in the micelles revealing microviscosity of the immediate probe environments and associated energetics. The strategy of investigating water dynamics in similar micellar systems using time-resolved dynamics Stokes shift is well documented in the literature.[25] Femtosecond resolved Stokes shifts of a well-known solvation probe C500 in the micelles have been followed for the investigation of hydration dynamics at the micellar surface. A coupling of the structural flexibility of the micelles with their dynamics of hydration is evident from our studies. We have also employed femtosecond resolved Förster resonance energy transfer (FRET) for the investigation of nonspecific binding of a cationic dye ethidium bromide (EtBr) salt to the micellar surface. A strong spectral overlap of the emission of C500 with the absorption spectrum of EtBr reveals the possibility of energy transfer from C500 (donor) to the acceptor EtBr through dipole−dipole coupling.[26] The distribution of the donor−acceptor distances in the micelles clearly reveals a correlation of the structural flexibility of the micelles in their molecular recognition by a small organic ligand (EtBr). Overall, our present study is an attempt to explore the coupling of structural flexibility with the dynamics of hydration of nanoscopic micellar systems using femtosecond to picosecond resolved electronic spectroscopy.

MATERIALS AND METHODS

Materials. Sodium dodecyl sulfate (SDS; $C_{12}H_{25}SO_4Na$) and sodium dodecylbenzenesulfonate (SDBS; $C_{12}H_{25}C_6H_4SO_3Na$) were products of Sigma (purity ≥99.0%). For QENS studies, micellar solution was prepared separately in D_2O (99.9% atom D purity) for both the surfactants. Coumarin 500 (C500) and ethidium bromide (EtBr) are from Exciton and Molecular Probes, respectively. The water is from Millipore system.

Optical Studies. Steady-state absorption and emission spectra of the corresponding systems are measured with Shimadzu UV-2450 spectrophotometer and Jobin Yvon Fluorolog fluorimeter, respectively. Femtosecond-resolved fluorescence is measured using a femtosecond upconversion setup (FOG 100, CDP) with full width at half-maximum (fwhm) of 185 fs. The samples were excited at 400 nm, and more details of the system can be found elsewhere.[27] Time-resolved emission spectrum (TRES) and solvent correlation function, $C(t)$, anisotropy $r(t)$, were constructed following earlier published work.[7,27,28] FRET distance between donor−acceptor (r) was calculated from the equation $r^6 = [R_0^6(1 - E)]/E$, where E is the energy transfer efficiency between donor and acceptor and following the procedure published elsewhere.[29] Distance distribution function $P(r)$ was calculated using nonlinear least-squares fitting procedure using SCIENTIST software to the following function $p(r) = \{1/[\sigma(2\pi)^{1/2})]\}\exp\{-^1/_2[(\bar{r} - r)/\sigma]^2\}$, where $\bar{r}$ is the mean of the Gaussian with a standard deviation of σ, and r is the donor−acceptor distance. Detailed theory and calculations of distance distribution can be found elsewhere.[29−31]

Dynamic Light Scattering (DLS). Hydrodynamic diameter (d_h) of the micelles was calculated using the equation $d_h = (k_BT)/(3\pi\eta D)$, in which k_B, η, and D are Boltzmann constant, viscosity, and translational diffusion coefficient, respectively, at absolute temperature T. Details of DLS setup and experiment can be found elsewhere.[32] Following modified Stokes−Einstein−Debye equation,[32] $\tau_r = (\eta_m V_m f C)/(k_B T)$ microviscosity (η_m) can be calculated, where τ_r is rotational time constant of the probe in the micelles and k_B and V_m are Boltzmann constant and molecular volume of the probe (198 Å^3) at absolute temperature T. C represents solute−solvent coupling constant, whereas f is the shape factor. Here we have considered the values of C and f to be unity.

Quasielastic Neutron Scattering (QENS). A 0.3 M micellar solution was prepared separately in D_2O (99.9% atom D purity) for both surfactants. Experiments were carried out using the IRIS time-of-flight spectrometer at the ISIS pulsed neutron facility, U.K. IRIS is an inelastic neutron scattering instrument that works on inverted geometry with an array of pyrolytic graphite analyzer crystals situated near backscattering geometry. PG (002) analyzer provides an elastic resolution of 17.5 μeV at a final energy of 1.84 meV over wave vector transfer (Q) range from 0.44 to 1.83 Å^{-1} with an energy window from 0.35 to 1.2 meV (in offset configuration). In order to achieve no more than 10% scattering, the samples were placed in a cylindrical aluminum can with an internal spacing of 1 mm. QENS measurements were carried out on a micellar solution in D_2O at temperatures of 300 K. Since we are interested in the dynamics of the micelles, we subtract the scattering contribution from D_2O after measuring the QENS spectra for pure D_2O. Data reduction involving background subtraction and detector efficiency corrections were performed by using the ISIS data analysis package, MODES.[33]

RESULTS AND DISCUSSION

Steady-State Optical Studies. Figure 1a shows steady state absorption and emission spectra of the probe (C500) in solvents of different degrees of polarity. The emission peak in cyclohexane at 417 nm moves to 510 nm in water. The absorption spectra of the probe in the two solvents do not show much change (data not shown) revealing significantly larger transition dipole moment upon excitation.[34] The emission maxima of the probe C500 in the SDS and SDBS micelles are found to be 505 and 508 nm, respectively, indicating the location of the probe at the micellar interface. Similar spectral width of the emission profiles of the probe C500 in the micellar media and bulk water rules out significant heterogeneity in the location of the probe in the micelles. A slight but reproducible shift of emission spectrum of the probe C500 in SDBS compared to that in SDS is indicative of more polar environment in the vicinity of the probe in SDBS micelle. Relatively higher steady state fluorescence anisotropy value of the probe C500 in SDBS micelle (~0.05) compared to that in SDS micelle (~0.03) is evident from Figure 1b, which suggests a more restricted environment of the probe in the former medium. The persistency of the steady state anisotropy values in a range of emission wavelengths (470−530 nm) in the micelles is also indicative of less heterogeneity in the probe's microenvironments in the micelles. Dynamics light scattering (DLS) experiments on the micelles (Figure 1c) reveals similar and almost monodispersed distribution of the SDS and SDBS

DOI: 10.1021/jp511899q
J. Phys. Chem. B XXXX, XXX, XXX−XXX

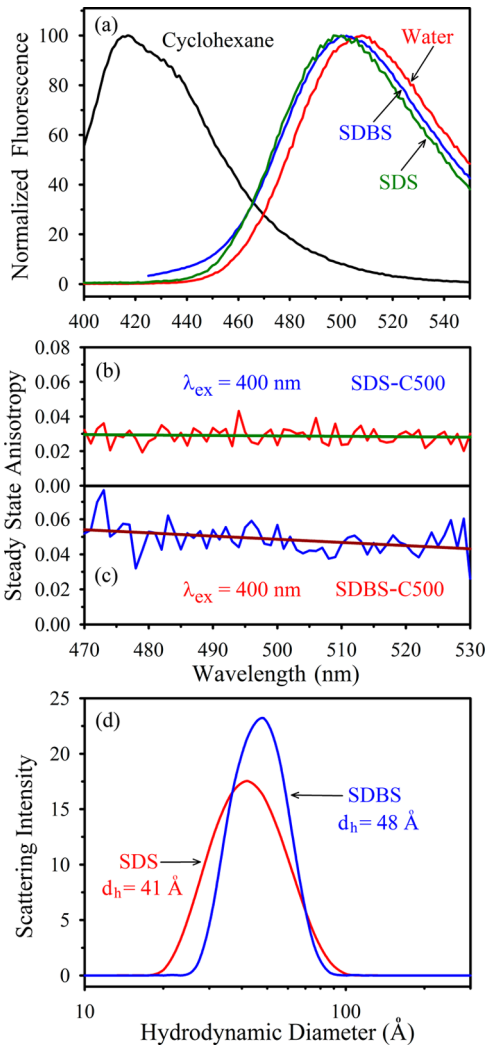

Figure 1. (a) Steady state emission spectra of fluorescence probe C500 in various solvent and in SDS and SDBS micelles. Steady state anisotropy of the probe in SDS and SDBS micelles are shown in (b) and (c) respectively. (d) Typical DLS spectra of both micelles showing their corresponding hydrodynamic diameter.

micelles with hydrodynamic diameters of 4.1 and 4.8 nm, respectively, consistent with earlier reported values.[35,36]

Quasielastic Neutron Scattering (QENS). Neutron scattering data from a micellar system have dominant contribution from hydrogen atoms present due to their high incoherent cross-section compared to other elements. The measured scattering intensity can therefore be written as[37]

$$I = \frac{\partial^2\sigma}{\partial\Omega\,\partial\omega} \propto \frac{k_i}{k_f}\sigma_{inc}\, S_{inc}(Q,\omega) \tag{1}$$

where $S_{inc}(Q,\omega)$ is the dynamical scattering function describing single particle motion. Here Q $(=k_i - k_f)$ is the wave vector transfer, k_i and k_f are the incident and scattered neutron wave vectors, respectively, and $\hbar\omega$ is the energy transfer. To minimize the scattering contribution from the solvent, deuterated water was used. In order to obtain the contribution from the micelles alone, data from the pure solvent were subtracted from that of the micellar solution. Figure 2 shows QENS spectra measured for SDS and SDBS micelles (contribution of D_2O subtracted) at Q = 1.0 Å^{-1}. Observed quasielastic broadening for SDS micelles is found to be

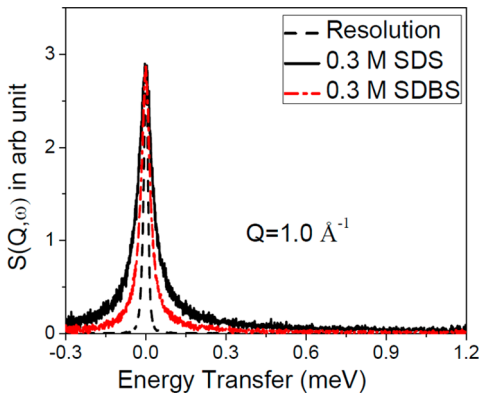

Figure 2. Typical QENS spectra for 0.3 M SDS and SDBS micellar solution at Q = 1.0 Å^{-1}. The instrument resolution is shown by dashed line. All the spectra are normalized to peak intensities.

significantly larger in SDS compared to SDBS, suggesting slower dynamics in SDBS compared to SDS micelle.

Varieties of motions are plausible in a micellar system, such as global motion (which includes translational and rotation of the micelles), internal motions of different CH_2 units, and fast torsional motion within the micelle.[38] It is these dynamical processes that are expected to contribute within the time scales of the neutron scattering technique used (10^{-9}–10^{-12} s). Therefore, QENS spectra shown in Figure 2 consist of all these motions, and to find out the contribution from different dynamical processes, we need to model the total dynamical scattering function. Assuming that these dynamical processes are independent of each other, the scattering law, $S_{micelles}(Q,\omega)$ can be expressed as a convolution of the global and internal motions of the micelles.[22] It may be noted that "global" motion of the micelle involves both translational and rotational motion of the whole micelle. It has been shown that the total scattering law comprising both translational and rotational motion can be described by a single Lorentzian function for dispersed spherical nanometer sized macromolecules.[39] Therefore, the scattering law for global motion can be written as[37]

$$S_G(Q,\omega) = L_G(\Gamma_G,\omega) = \frac{1}{\pi}\frac{\Gamma_G}{\Gamma_G^{\,2} + \omega^2} \tag{2}$$

Here Γ_G is the half width at half maxima (hwhm) of the Lorentzian function corresponding to global motion and is proportional to the global diffusivity, D_G, of the micelles. Perez et al.[39] have also showed numerically that the D_G, obtained with single Lorentzian description, is higher compared to the self-diffusion coefficient, D_s.

Apart from the global motion the data also have contribution from internal motion of the surfactant monomers. This scattering law consists of an elastic component and a quasielastic component. The scattering law for the internal motion, $S_{in}(Q,\omega)$ can be expressed as[22]

$$S_{in}(Q,\omega) = A(Q)\,\delta(\omega) + (1 - A(Q))\,L_{in}(\Gamma_{in},\omega) \tag{3}$$

The quasielastic component is approximated as a single Lorentzian function, $L_{in}(\Gamma_{in},\omega)$ with hwhm, Γ_{in}. Elastic incoherent structure factor (EISF),[22] defined as the fraction of the elastic scattering out of total scattering, is useful to understand the geometry of a dynamical motion and can be identified as $A(Q)$ in eq 3. As mentioned above, the scattering law for micelles is the convolution product of the global and internal motions, which can be written as[22]

DOI: 10.1021/jp511899q
J. Phys. Chem. B XXXX, XXX, XXX−XXX

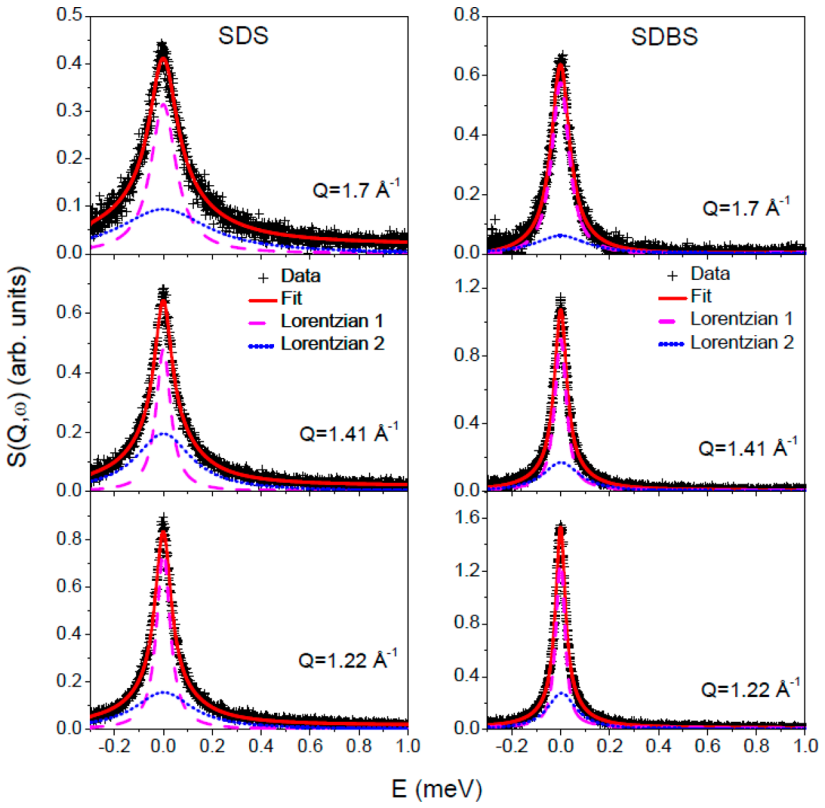

Figure 3. Typical fitted $S(Q,\omega)$ for 0.3 M SDS and SDBS micelles at different Q values, assuming the scattering function given in eq 4.

$$S_{\text{micelles}}(Q,\omega) = [A(Q)\, L_G(\Gamma_G,\omega) + (1 - A(Q))\, L_{\text{tot}}(\Gamma_{\text{tot}},\omega)] \quad (4)$$

Here, L_{tot} $(\Gamma_{\text{tot}},\omega)$ represents the total contribution from global and internal motions and $\Gamma_{\text{tot}} = \Gamma_G + \Gamma_{\text{in}}$. The program DAVE[40] developed at the NIST Center for Neutron Research is used to analyze the QENS data. The parameters $A(Q)$, Γ_G, and Γ_{tot} are obtained by least-squares fit with the measured data after convoluting the above scattering law (eq 4) with the instrumental resolution function. It is found that the model function (eq 4) could fit the observed QENS spectra very well at all the Q values. Typical fitted spectra for SDS and SDBS micelles are shown in Figure 3 at some typical Q values. The variation of the hwhm, Γ_G, of the first Lorentzian for SDBS is shown in Figure 4a along with that of SDS micelles. Larger Γ_G for SDS suggests that the global motion is faster in SDS than SDBS micelles. It is clear that the global diffusion follows Fick's law ($\Gamma_G = D_G Q^2$, D_G being the global diffusion coefficient) for both micellar systems as shown by solid lines in Figure 4a. $D_G = (1.9 \pm 0.3) \times 10^{-6}$ is obtained for SDBS, whereas for SDS micelle, it is found to be $(3.4 \pm 0.4) \times 10^{-6}$ cm^2/s.[22] Self-diffusion constant for pure translational motion of the micelles, D_s, can be calculated using Stokes–Einstein relation, $D_s = k_B T/(6\pi\eta R)$. Here R is the hydrodynamic radius of micelles, η, the viscosity of D_2O, and T, the temperature of the solution. For SDS micelles having radius $R = 20.5$ Å, $\eta_{D2O} = 0.9$ cP [41] at $T = 300$ K, the value of D_s obtained as 1.2×10^{-6} cm^2/s which is between the value reported by Hayter and Penfold[42] and the present work. Although several studies including MD simulation studies[21] on SDS and SDBS estimated the similar sizes of SDS and SDBS micelle, global diffusivities obtained from QENS study are found to be significantly different in SDS and SDBS micelles.

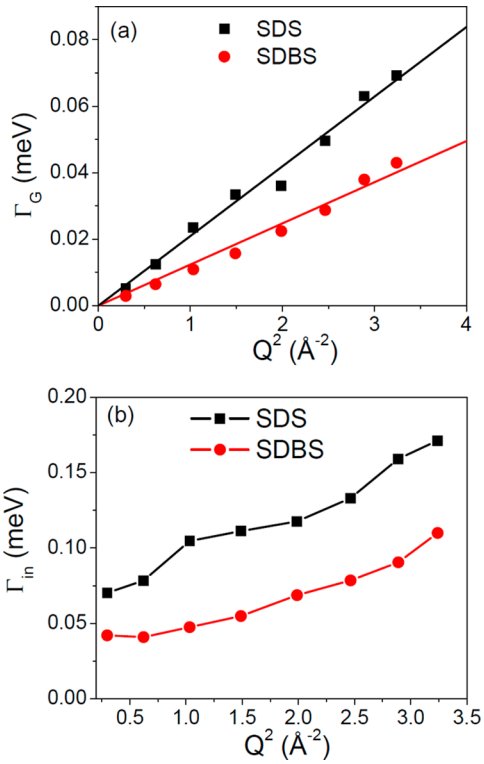

Figure 4. (a) Variation of half width at half maxima (hwhm), Γ_G, corresponds to global motion, with Q^2 for SDBS and SDS micelles. (b) Variation of the hwhm, Γ_{in}, which corresponds to the internal motion of the monomer for SDS and SDBS micelle with Q^2.

DOI: 10.1021/jp511899q
J. Phys. Chem. B XXXX, XXX, XXX−XXX

Γ_{in} corresponding to internal motion is obtained by subtracting Γ_G (as already known from the first Lorentzian in eq 4) from Γ_{tot}. The values of Γ_{in} obtained for SDS and SDBS are shown in Figure 4b. It is evident from the figure that the internal motion is faster in SDS than SDBS. More compact or denser hydrophobic core of the SDBS micelle compared to SDS micelle leads to the constriction in the internal motion in SDBS micelle. As stated earlier, the π stacking between the aromatic rings of the adjacent surfactants is one of the possibilities for the compactness. In effect, more "viscous" (dense) medium in SDBS micelle (because of increase in packing density) provides the basis for constrained dynamics of mobile protons in SDBS than in SDS.

The obtained $A(Q)$, which represents the EISF for the internal motion for both of the micelles, is shown in Figure 5. It is evident that the EISFs for SDBS micelles are higher than that of SDS micelles, indicating that alkyl chains in SDS are more dynamic than in SDBS micelles. The main feature of the internal motions in a structured system is the confinement of the species within a certain volume of space. The exact shape of this volume is not well-known but in a first approximation is assumed as spherical. Volino and Dianoux[43] had derived the scattering law for diffusion of particles within a sphere with an impermeable surface. It may be noted that all the hydrogen atoms might not be dynamically active at a given temperature, considering the same, a factor P_x is introduced, representing fraction of hydrogen atoms which are dynamically inactive at a given temperature. This methodology is widely used in a number of systems including vesicles,[44] proteins,[39] hemoglobin,[45] etc. to describe the hydrogen mobility in long chain systems. The modified EISF can then be written as

$$\text{EISF} = P_x + (1 - P_x)\left[\frac{3j_1(Qa)}{(Qa)}\right]^2 \quad (5)$$

Here, $j_1(Qa)$ is the spherical Bessel function of the first order and a is the radius of the confining volume. Solid lines in Figure 5 shows the least-squares fit of the experimentally obtained EISF using the above equation. It is found that in the case of SDS micelles, about 48(±2)% of the hydrogen atoms are dynamically inactive, while in case of SDBS micelles it is about 62(±2)%. The radius of confinement for both SDS and SDBS is found to be 2.9(±0.2)Å. This suggests that the spatial domain of dynamics of the hydrogen atoms is ∼6 Å in both micellar systems.

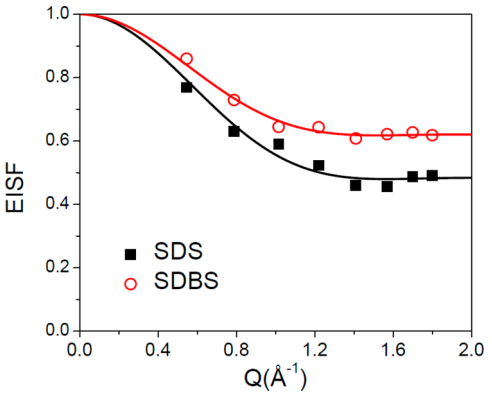

Figure 5. Variation of EISF for SDS and SDBS micellar solution with Q. Solid lines are fitted curves assuming eq 5.

Polarization-Gated Fluorescence Anisotropy. In order to investigate the physical movement of the probe C500 molecule in the micelles during the course of hydration relaxation around the probe, we have measured the fluorescence anisotropy of the probe in the micelles as shown in Figure 6a,b. The fluorescence anisotropy decays depict rotational relaxation time constants of C500 in SDS and SDBS micelles of 283 and 342 ps, respectively. The observed time constants are much slower and are consistent with those measured from picoseconds resolved time correlated single photon counting (TCSPC) technique. In order to calculate π-

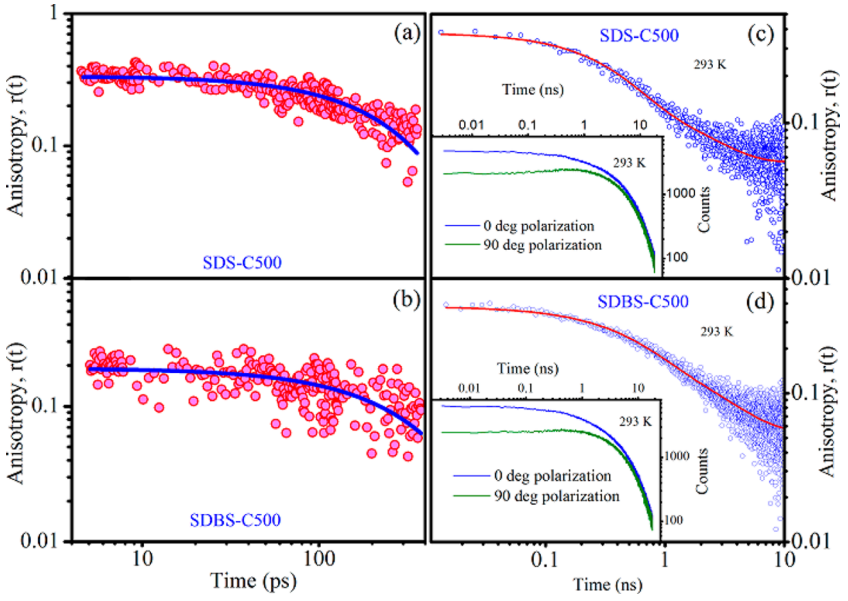

Figure 6. Femtosecond fluorescence anisotropy decays of C500 in SDS (a) and SDBS (b) are shown in log−log plot. The room temperature picoseconds resolved anisotropy of C500 in SDS (c) and SDBS (d) are also shown. Inserts shows parallel and perpendicular polarization gated decays for the corresponding systems.

DOI: 10.1021/jp511899q
J. Phys. Chem. B XXXX, XXX, XXX−XXX

stacking energy in the case of SDBS micelle, we have measured temperature dependent anisotropy of both the micelles with TCSPC. Figure 6c,d shows the anisotropy decay of the probe in SDS and SDBS micelle at 293 K temperature, respectively. The corresponding parallel and perpendicular polarization gated decays are shown in the respective insets. Anisotropy at 278 and 343 K of both the SDS and SDBS micelle are shown in the inset of Figure 7a,b, respectively. As observed from Figure 7a,b

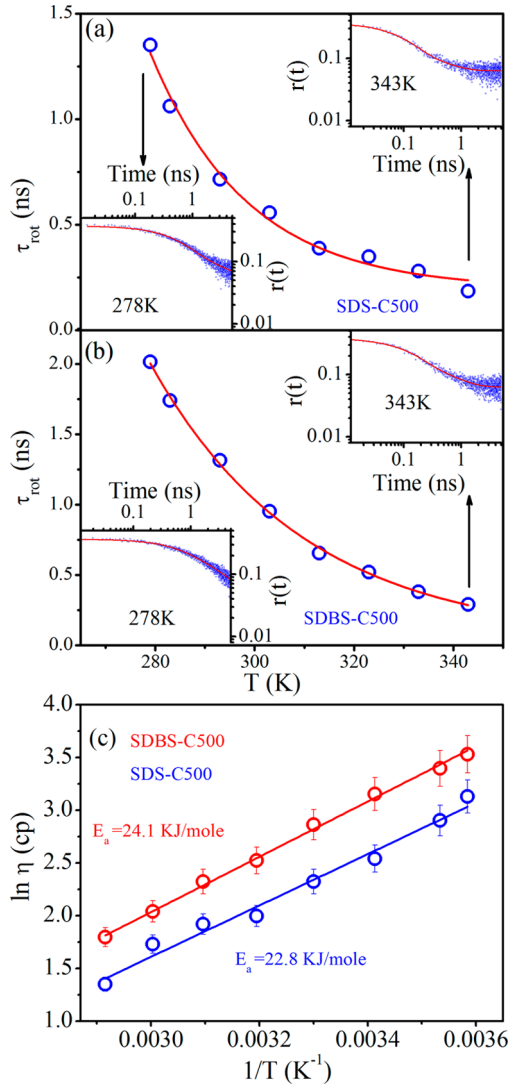

Figure 7. Plot of rotational time constant (τ_{rot}) against temperature for SDS (a) and SDBS (b) micelle. Inserts are showing anisotropy at initial and final temperature for the respective systems. (c) Arrhenius plots of microviscosity for SDS and SDBS micelles are shown (with 5% error bar).

rotational time constant (τ_{rot}) becomes faster upon increasing temperature for both systems. We have estimated micro-viscosities at different temperature for the corresponding systems, given the hydrodynamics diameter of the probe is 7.6 Å as reported earlier[32] and plotted with $1/T$ (K^{-1}) as shown in Figure 7c. The plots are distinct and out of the experimental uncertainty (5%). Linear fit of both plots provide activation energy 22.8(±1.1) kJ/mol and 24.1(±1.2) kJ/mol for SDS and SDBS, respectively, using the equation[46] $\eta = \eta_0 \exp[E_\eta/(RT)]$, where E_η is the energy barrier for viscous flow. The relatively higher activation energy in the SDBS micelles compared to that in SDS micelle is probably the manifestation of less flexibility of the alkyl chains due to π-stacking (1.3 kJ/mol) in the former medium.[47]

Femtosecond-Resolved Dynamics of Hydration. To correlate the fluctuations with hydration dynamics of the micelles, we have performed femtosecond solvation dynamics of both micelles. The femtosecond resolved fluorescence transients of C500 in SDS and SDBS micelles at three characteristic wavelengths (440, 480, and 560 nm) across the emission wavelengths are shown in Figure 8a and Figure 8b,

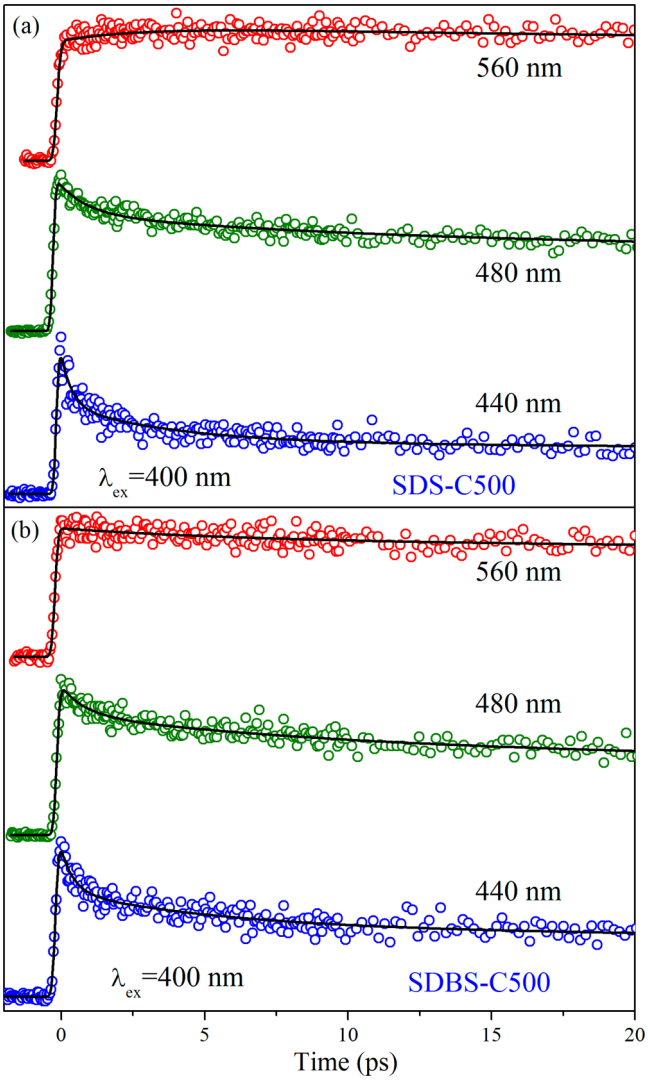

Figure 8. Femtosecond resolved fluorescence transients of C500 in three representative detection wavelengths (440, 480, and 560 nm) for SDS (a) and SDBS (b) micelles are shown. The circles are experimental data, and the solid lines are best multiexponential fit (see text).

respectively. An ultrafast decay component in the blue end is eventually converted into a rise component of similar time constant in the red end for both the micelles. The observation is consistent with the solvation of the probe C500 in the media.[24] The constructed time dependent Stokes shifts (TDSSs) of the C500 emission at different times are shown in Figure 9a and Figure 9b, with a spectral shift of 1260 and 1080 cm^{-1} for SDS and SDBS micelles, respectively, in a 1 ns time window. The hydration correlation functions [$C(t)$] for

DOI: 10.1021/jp511899q
J. Phys. Chem. B XXXX, XXX, XXX−XXX

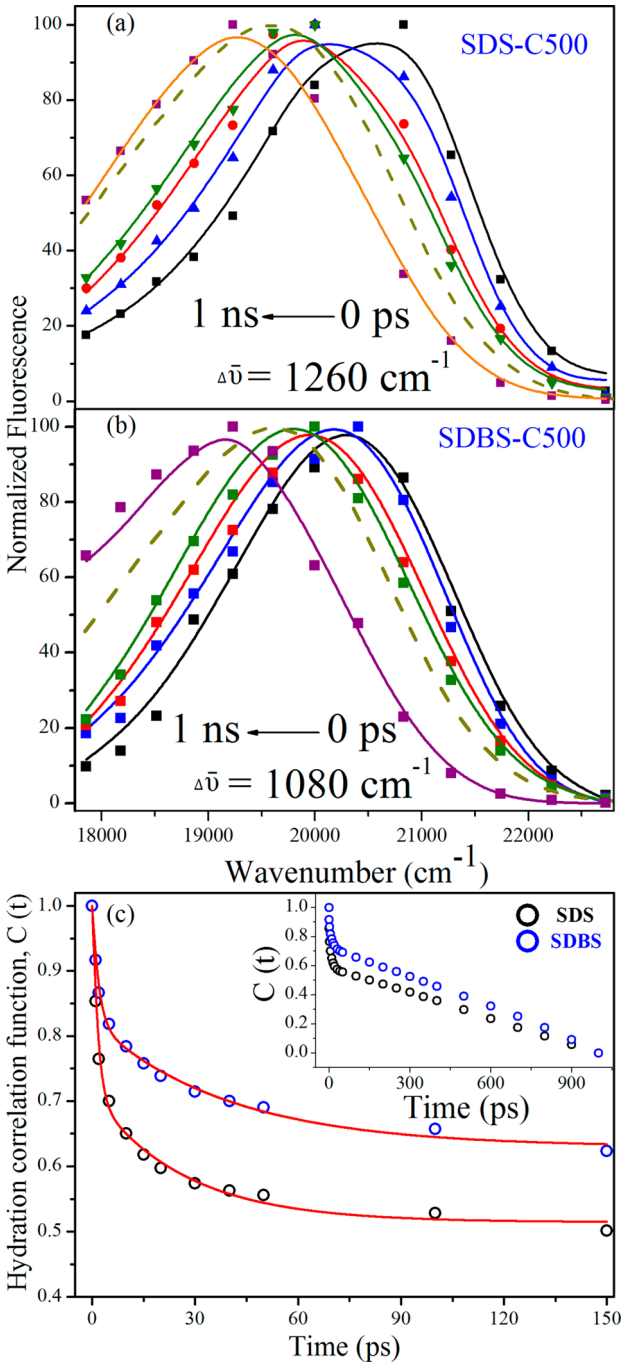

Figure 9. Time dependent emission spectra (TRES) of fluorescent probe C500 in SDS (a) and SDBS (b) micelles are shown. The dotted lines are the steady state fluorescence spectra of the corresponding systems. $\Delta\bar{\nu}$ is the spectral shift for the micellar system in 1 ns time window. (c) Hydration correlation functions for the SDS and SDBS are shown up to 150 ps. The solid lines are the best biexponential fit to $C(t)$. Inset shows the correlation function in long time range.

the SDS and SDBS micelles up to 150 ps as shown in Figure 9c can be fitted with biexponential decay functions. $C(t)$ up to 1 ns for SDS and SDBS as shown in inset is nonexponential because of contribution of fluctuation of the micellar headgroup. Up to 150 ps for SDS micelles the decay time constants are 1.48 ps (59%) and 27 ps (41%), and for SDBS micelles the obtained time constants are 1.75 ps (48%) and 39 ps (52%). Our result is consistent with earlier femtosecond resolved study[48] on the dynamics of hydration in TX-100 micelle reported hydration time constants of 2.9 ps (45%) and 58 ps (55%).[49] It has to be noted that the correlation functions for both micelles show nonexponential behavior after 150 ps up to a time window of 1 ns. The nonexponential behavior of biologically relevant macromolecules including DNA has been well documented at a time window from femtosecond until microsecond.[50] Earlier it has been concluded that the faster response in the $C(t)$ is a consequence of the movement of counterions away from their average position through the electric field at the probe. On the other hand relatively slower components are from various kinds of motions of the host system itself.[50,51] Overall, a variety of dynamical events are likely to be included in the solvation response and the relaxation dynamics must be treated as a collective response of the whole system. The faster dynamics of hydration in SDS than that in SDBS micelle is clearly evident from the study. The structural flexibility of the SDS and SDBS micelles is also evident from polarization gated fluorescence anisotropy studies (Figure 6), revealing higher rigidity in the latter case. Thus, our observation of faster hydration dynamics in structurally flexible SDS micelle may find a correlation between the dynamics of hydration water and internal motion of the micelles.

Femtosecond-Resolved Förster Resonance Energy Transfer (FRET). In Figure 10 we have shown the molecular complexation of a cationic dye EtBr with the anionic micelles SDS and SDBS using FRET techniques.[52] Figure 10a shows the overlap (overlap integral value of 3.37×10^{14} M^{-1} cm^{-1} nm^4) between the emission spectrum of C500 (donor) and the absorption spectrum of EtBr (acceptor) in the SDS micelle. The overlap for the SDBS micelles remains almost unchanged (overlap integral value of 3.1×10^{14} M^{-1} cm^{-1} nm^4; data not shown in the figure). Femtosecond resolved fluorescence transients of C500 at 500 nm in the micelles before and after the complexation with the acceptor EtBr is shown in the Figure 10b and Figure 10c. A significant faster component of 409 fs (32%) in the case of SDS micelles upon complexation with EtBr is clearly evident. In the case of SDBS micelle the faster component is found to be 475 fs (10%). The estimated Förster distance (R_0) values of the donor–acceptor pair for the SDS and SDBS micelles are 34.61 and 34.14 Å, respectively. The calculated donor–acceptor distances in the two micelles are found to be 33.64 and 45.0 Å, respectively. The higher donor–acceptor distance in the case of SDBS compared to that in SDS micelle may not be due to the distant location of the donor C500 from the micellar surface, as the fluorescence spectrum of the donor probe shows similar characteristics revealing insignificant change in the polarity around the probe. In the case of deep insertion of the probe from the surface, lower polarity around the probe is unavoidable. Thus, the observation can be rationalized in terms of different position of the acceptor EtBr at the surface of the SDBS micelle compared to that of the SDS. The intrinsic micellar fluctuation, as evidenced in microviscosity (described above), is also substantiated in our FRET studies on the molecular recognition of EtBr by the two micellar systems. The distribution of donor–acceptor distances in the micelles is also shown in Figure 10d revealing relatively less broadening in the case of SDBS (half width of 2.5 Å) compared to that in SDS (half width of 3.4 Å). The observation of high width in the donor–acceptor distance distribution in case of SDS micelle compared to SDBS micelle can be rationalized in terms of dynamical fluctuation of the host micelles.[31,53] The calculated half width values, revealing

DOI: 10.1021/jp511899q
J. Phys. Chem. B XXXX, XXX, XXX–XXX

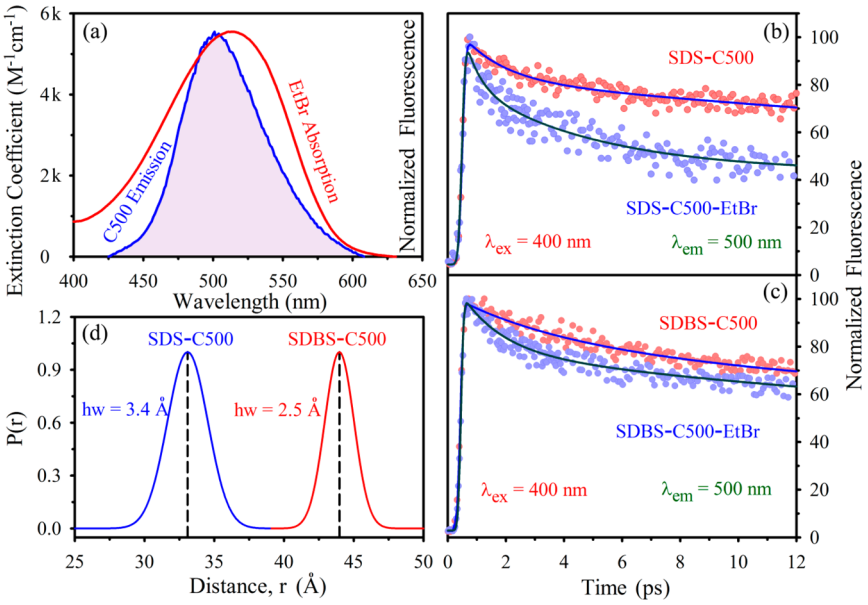

Figure 10. Spectral overlap of C500 emission and EtBr absorption in SDS micelles is shown in (a). (b) and (c) show fluorescence transient of C500 in the micelles at 500 nm before and after complexation with cationic dye EtBr. (d) shows distribution of donor−acceptor distances in the two micelles.

heterogeneity or fluctuation in the observed distances between the donor and the acceptor, thus correlated with the dynamics of hydration.

CONCLUSION

Here we employed femtosecond resolved electronic spectroscopy for the exploration of hydration dynamics of a well-known solvation probe C500 in two structurally similar anionic micelles SDS and SDBS. Dynamic light scattering (DLS) reveals the structural integrity of the micelles. We have used polarization gated fluorescence anisotropy for the estimation of structural flexibility of the micelles. We have found SDBS is more compact than SDS. The extracted dynamics of hydration in the micelles reveal slower water motion at the less flexible SDBS micelle compared to that in SDS micelle. The comparison of the dynamics of hydration across two micelles of different compactness reveals a gradient of coupling between hydration water and internal micellar motions, which is stronger in relatively flexible SDS and weaker in compact SDBS micelles. Slower internal motion in SDBS compared to SDS micelle is also confirmed from QENS studies. We have also used femtosecond resolved FRET in order to investigate the molecular recognition of the micelles by a small cationic ligand EtBr. Relatively broad distribution of EtBr at the micellar surfaces with respect to the probe C500 in the case of SDS micelle compared to that in SDBS micelle is evident. The observation is correlated with the internal flexibility of the micelles. Thus, our present study can be considered as an exploration of a coherent picture of structure, dynamics, and function of molecular recognition at physiologically relevant important nanoscopic micellar environments.

AUTHOR INFORMATION

Corresponding Author

*E-mail:skpal@bose.res.in.

Notes

The authors declare no competing financial interest.

ACKNOWLEDGMENTS

S.C. thanks CSIR, India, for the research fellowships. Financial grants SB/S1/PC-011/2013 and DST/TM/SERI/2k11/103 from DST (India) and Grant 2013/37P/73/BRNS from DAE (India) are gratefully acknowledged.

REFERENCES

(1) Pal, S. K.; Zewail, A. H. Dynamics of Water in Biological Recognition. *Chem. Rev.* **2004**, *104*, 2099−2124.
(2) Ball, P. Water as an Active Constituent in Cell Biology. *Chem. Rev.* **2008**, *108*, 74−108.
(3) Wang, L.; Yu, X.; Hu, P.; Broyde, S.; Zhang, Y. A Water-Mediated and Substrate-Assisted Catalytic Mechanism for Sulfolobus Solfataricus DNA Polymerase IV. *J. Am. Chem. Soc.* **2007**, *129*, 4731−4737.
(4) Zong, C.; Papoian, G. A.; Ulander, J.; Wolynes, P. G. Role of Topology, Nonadditivity, and Water-Mediated Interactions in Predicting the Structures of alpha/beta Proteins. *J. Am. Chem. Soc.* **2006**, *128*, 5168−5176.
(5) Pechstedt, K.; Whittle, T.; Baumberg, J.; Melvin, T. Photoluminescence of Colloidal Cdse/Zns Quantum Dots: The Critical Effect of Water Molecules. *J. Phys. Chem. C* **2010**, *114*, 12069−12077.
(6) Migliore, A.; Corni, S.; Di Felice, R.; Molinari, E. Water-Mediated Electron Transfer between Protein Redox Centers. *J. Phys. Chem. B* **2007**, *111*, 3774−3781.
(7) Choudhury, S.; Batabyal, S.; Mondol, T.; Sao, D.; Lemmens, P.; Pal, S. K. Ultrafast Dynamics of Solvation and Charge Transfer in a DNA-Based Biomaterial. *Chem.—Asian J.* **2014**, *9*, 1395−1402.
(8) Rupley, J. A.; Careri, G. Protein Hydration and Function. *Adv. Protein Chem.* **1991**, *41*, 37−172.
(9) Kornblatt, J.; Kornblatt, M. Water as It Applies to the Function of Enzymes. *Int. Rev. Cytol.* **2002**, *215*, 49−73.
(10) Levy, Y.; Onuchic, J. N. Water Mediation in Protein Folding and Molecular Recognition. *Annu. Rev. Biophys. Biomol. Struct.* **2006**, *35*, 389−415.
(11) Kim, S. J.; Born, B.; Havenith, M.; Gruebele, M. Real-Time Detection of Protein−Water Dynamics upon Protein Folding by Terahertz Absorption Spectroscopy. *Angew. Chem., Int. Ed.* **2008**, *47*, 6486−6489.
(12) Zhou, F.; Schulten, K. Molecular Dynamics Study of a Membrane−Water Interface. *J. Phys. Chem.* **1995**, *99*, 2194−2207.

DOI: 10.1021/jp511899q
J. Phys. Chem. B XXXX, XXX, XXX−XXX

(13) Helms, V. Protein Dynamics Tightly Connected to the Dynamics of Surrounding and Internal Water Molecules. *ChemPhysChem* **2007**, *8*, 23−33.
(14) Bhattacharyya, K. Nature of Biological Water: A Femtosecond Study. *Chem. Commun.* **2008**, 2848−2857.
(15) Gallat, F.-X.; Laganowsky, A.; Wood, K.; Gabel, F.; Van Eijck, L.; Wuttke, J.; Moulin, M.; Härtlein, M.; Eisenberg, D.; Colletier, J.-P. Dynamical Coupling of Intrinsically Disordered Proteins and Their Hydration Water: Comparison with Folded Soluble and Membrane Proteins. *Biophys. J.* **2012**, *103*, 129−136.
(16) Qvist, J.; Ortega, G.; Tadeo, X.; Millet, O.; Halle, B. Hydration Dynamics of a Halophilic Protein in Folded and Unfolded States. *J. Phys. Chem. B* **2012**, *116*, 3436−3444.
(17) Conti Nibali, V.; D'Angelo, G.; Paciaroni, A.; Tobias, D. J.; Tarek, M. On the Coupling between the Collective Dynamics of Proteins and Their Hydration Water. *J. Phys. Chem. Lett.* **2014**, *5*, 1181−1186.
(18) Heyden, M.; Tobias, D. J. Spatial Dependence of Protein-Water Collective Hydrogen-Bond Dynamics. *Phys. Rev. Lett.* **2013**, *111*, 218101.
(19) Tarek, M.; Tobias, D. J. Single-Particle and Collective Dynamics of Protein Hydration Water: A Molecular Dynamics Study. *Phys. Rev. Lett.* **2002**, *89*, 275501.
(20) Pal, S. K.; Zhao, L.; Zewail, A. H. Water at DNA Surfaces: Ultrafast Dynamics in Minor Groove Recognition. *Proc. Natl. Acad. Sci. U.S.A.* **2003**, *100*, 8113−8118.
(21) Palazzesi, F.; Calvaresi, M.; Zerbetto, F. A Molecular Dynamics Investigation of Structure and Dynamics of Sds and Sdbs Micelles. *Soft Matter* **2011**, *7*, 9148−9156.
(22) Sharma, V.; Mitra, S.; Johnson, M.; Mukhopadhyay, R. Dynamics in Anionic Micelles: Effect of Phenyl Ring. *J. Phys. Chem. B* **2013**, *117*, 6250−6255.
(23) Islam, M.; Rojas, E.; Bergey, D.; Johnson, A.; Yodh, A. High Weight Fraction Surfactant Solubilization of Single-Wall Carbon Nanotubes in Water. *Nano Lett.* **2003**, *3*, 269−273.
(24) Rakshit, S.; Saha, R.; Verma, P. K.; Pal, S. K. Role of Solvation Dynamics in Excited State Proton Transfer of 1-Naphthol in Nanoscopic Water Clusters Formed in a Hydrophobic Solvent. *Photochem. Photobiol.* **2012**, *88*, 851−859.
(25) Nandi, N.; Bhattacharyya, K.; Bagchi, B. Dielectric Relaxation and Solvation Dynamics of Water in Complex Chemical and Biological Systems. *Chem. Rev.* **2000**, *100*, 2013−2046.
(26) Majumder, P.; Sarkar, R.; Shaw, A. K.; Chakraborty, A.; Pal, S. K. Ultrafast Dynamics in a Nanocage of Enzymes: Solvation and Fluorescence Resonance Energy Transfer in Reverse Micelles. *J. Colloid Interface Sci.* **2005**, *290*, 462−474.
(27) Banerjee, D.; Makhal, A.; Pal, S. K. Sequence Dependent Femtosecond-Resolved Hydration Dynamics in the Minor Groove of DNA and Histone—DNA Complexes. *J. Fluoresc.* **2009**, *19*, 1111−1118.
(28) Horng, M. L.; Gardecki, J. A.; Papazyan, A.; Maroncelli, M. Subpicosecond Measurements of Polar Solvation Dynamics: Coumarin 153 Revisited. *J. Phys. Chem.* **1995**, *99*, 17311−17337.
(29) Batabyal, S.; Mondol, T.; Choudhury, S.; Mazumder, A.; Pal, S. K. Ultrafast Interfacial Solvation Dynamics in Specific Protein DNA Recognition. *Biochimie* **2013**, *95*, 2168−2176.
(30) Lakowicz, J. R.; Geddes, C. D. *Topics in Fluorescence Spectroscopy*; Springer: New York, 1991; Vol. *1*.
(31) Chaudhuri, S.; Batabyal, S.; Polley, N.; Pal, S. K. Vitamin B2 in Nanoscopic Environments under Visible Light: Photosensitized Antioxidant or Phototoxic Drug? *J. Phys. Chem. A* **2014**, *118*, 3934−3943.
(32) Banerjee, D.; Verma, P. K.; Pal, S. K. Temperature-Dependent Femtosecond-Resolved Hydration Dynamics of Water in Aqueous Guanidinium Hydrochloride Solution. *Photochem. Photobiol. Sci.* **2009**, *8*, 1441−1447.
(33) Howells, W. S.; Garcia Sakai, V.; Demmel, F.; Telling, M. T. F.; Fernandez-Alonso, F. *The MODES User Guide*, version 3; Rutherford Appleton Laboratory: Didcot, U.K., 2010.
(34) Lewis, J.; Maroncelli, M. On the (Uninteresting) Dependence of the Absorption and Emission Transition Moments of Coumarin 153 on Solvent. *Chem. Phys. Lett.* **1998**, *282*, 197−203.
(35) Bruce, C. D.; Berkowitz, M. L.; Perera, L.; Forbes, M. D. Molecular Dynamics Simulation of Sodium Dodecyl Sulfate Micelle in Water: Micellar Structural Characteristics and Counterion Distribution. *J. Phys. Chem. B* **2002**, *106*, 3788−3793.
(36) Cheng, D. C.; Gulari, E. Micellization and Intermicellar Interactions in Aqueous Sodium Dodecyl Benzene Sulfonate Solutions. *J. Colloid Interface Sci.* **1982**, *90*, 410−423.
(37) Bee, M. *Quasielastic Neutron Scattering*; Adam Hilger: Bristol, U.K., 1988.
(38) Sharma, V. K.; Mitra, S.; Garcia Sakai, V.; Hassan, P. A.; Peter Embs, J.; Mukhopadhyay, R. The Dynamical Landscape in CTAB Micelles. *Soft Matter* **2012**, *8*, 7151−7160.
(39) Pérez, J.; Zanotti, J.-M.; Durand, D. Evolution of the Internal Dynamics of Two Globular Proteins from Dry Powder to Solution. *Biophys. J.* **1999**, *77*, 454−469.
(40) Azuah, R. T.; Kneller, L. R.; Qiu, Y.; Tregenna-Piggott, P. L.; Brown, C. M.; Copley, J. R.; Dimeo, R. M. DAVE: A Comprehensive Software Suite for the Reduction, Visualization, and Analysis of Low Energy Neutron Spectroscopic Data. *J. Res. Natl. Inst. Stand. Technol.* **2009**, *114*, 341−358.
(41) Castelletto, V.; Hamley, I. W.; Yang, Z.; Haeussler, W. Neutron Spin-Echo Investigation of the Dynamics of Block Copolymer Micelles. *J. Chem. Phys.* **2003**, *119*, 8158−8161.
(42) Hayter, J. B.; Penfold, J. *J. Chem. Soc., Faraday Trans. 1* **1981**, *77*, 1851−1863.
(43) Volino, F.; Dianoux, A. Neutron Incoherent Scattering Law for Diffusion in a Potential of Spherical Symmetry. *J. Mol. Phys.* **1980**, *41*, 271−279.
(44) Gerelli, Y.; Sakai, V. G.; Ollivier, J.; Deriu, A. Conformational and Segmental Dynamics in Lipid-Based Vesicles. *Soft Matter* **2011**, *7*, 3929−3935.
(45) Caronna, C.; Natali, F.; Cupane, A. Incoherent Elastic and Quasi-Elastic Neutron Scattering Investigation of Hemoglobin Dynamics. *Biophys. Chem.* **2005**, *116*, 219−225.
(46) Mitra, R. K.; Verma, P. K.; Pal, S. K. Exploration of the Dynamical Evolution and the Associated Energetics of Water Nanoclusters Formed in a Hydrophobic Solvent. *J. Phys. Chem. B* **2009**, *113*, 4744−4750.
(47) Huber, R. G.; Margreiter, M. A.; Fuchs, J. E.; von Grafenstein, S.; Tautermann, C. S.; Liedl, K. R.; Fox, T. Heteroaromatic π-Stacking Energy Landscapes. *J. Chem. Inf. Model.* **2014**, *54*, 1371−1379.
(48) Pal, S. K.; Peon, J.; Zewail, A. H. Biological Water at the Protein Surface: Dynamical Solvation Probed Directly with Femtosecond Resolution. *Proc. Natl. Acad. Sci. U.S.A.* **2002**, *99*, 1763−1768.
(49) Pal, S. K.; Sukul, D.; Mandal, D.; Sen, S.; Bhattacharyya, K. Solvation Dynamics of Dcm in Micelles. *Chem. Phys. Lett.* **2000**, *327*, 91−96.
(50) Andreatta, D.; Pérez Lustres, J. L.; Kovalenko, S. A.; Ernsting, N. P.; Murphy, C. J.; Coleman, R. S.; Berg, M. A. Power-Law Solvation Dynamics in DNA over Six Decades in Time. *J. Am. Chem. Soc.* **2005**, *127*, 7270−7271.
(51) Brauns, E. B.; Madaras, M. L.; Coleman, R. S.; Murphy, C. J.; Berg, M. A. Complex Local Dynamics in DNA on the Picosecond and Nanosecond Time Scales. *Phys. Rev. Lett.* **2002**, *88*, 158101.
(52) Pal, S. K.; Mandal, D.; Bhattacharyya, K. Photophysical Processes of Ethidium Bromide in Micelles and Reverse Micelles. *J. Phys. Chem. B* **1998**, *102*, 11017−11023.
(53) Nag, S.; Sarkar, B.; Chandrakesan, M.; Abhyanakar, R.; Bhowmik, D.; Kombrabail, M.; Dandekar, S.; Lerner, E.; Haas, E.; Maiti, S. A Folding Transition Underlies the Emergence of Membrane Affinity in Amyloid-B. *Phys. Chem. Chem. Phys.* **2013**, *15*, 19129−19133.

DOI: 10.1021/jp511899q
J. Phys. Chem. B XXXX, XXX, XXX−XXX